Astron. Astrophys. 333, 117–124 (1998)

ASTRONOMY AND ASTROPHYSICS

Globular clusters within 5° of the Galactic center⋆

B. Barbuy[1], **E. Bica**[2], **and S. Ortolani**[3]

[1] Universidade de São Paulo, CP 3386, Departamento de Astronomia, São Paulo 01060-970, Brazil
[2] Universidade Federal do Rio Grande do Sul, Departamento de Astronomia, CP 15051, Porto Alegre 91500-970, Brazil
[3] Università di Padova, Dipartimento di Astronomia, Vicolo dell'Osservatorio 5, I-35122 Padova, Italy

Received 1 April 1997 / Accepted 28 November 1997

Abstract. In the recent years we have concentrated efforts to collect Colour-Magnitude Diagrams of the globular clusters projected in the central parts of the Galaxy. So far we were able to gather photometric data in the V, I and Gunn z bandpasses, for 16 out of the 17 known clusters in the central 5° radius, most of them severely reddened. Reddening, distance and metallicity are estimated from the horizontal and red giant branches.

We study the resulting cluster spatial distribution and conclude that essentially no cluster is detected beyond the Galactic Center distance. The results favour a flattened bulge extending from the Galactic Center to 4.5 kpc from the Sun. The density distribution of the clusters follows the current models for bulge field stars. We estimate that missing clusters on the opposite side of the Galaxy bulge may amount ~ 15 clusters similar to those detected on our side. The projected distribution of clusters is asymmetrical, with higher absorption in the southern Galactic hemisphere. The metallicity distribution of our sample clusters results similar to that of bulge field stars.

The present ground-based results coupled to main sequence data of two genuine bulge clusters using the Hubble Space Telescope, point to a scenario of an old flat bulge with common origin for the stellar populations in both globular clusters and field.

Key words: globular clusters: general – Galaxy: center – Galaxy: formation – Hertzsprung–Russel (HR) and C-M diagrams

1. Introduction

The knowledge of age and spatial distribution of stars in the Galactic bulge require observational constraints to establish whether its stellar population is very old (Larson 1990) or is a younger, disk-like component (Raha et al. 1992), and if its shape is spherical or extended, or perhaps a bar (Spergel et al. 1996). Yet other possibilities are a flattened bulge or a disk-like system (Zinn 1985; Armandroff 1989; Ortolani et al. 1993b; Minniti 1995).

Until recently hardly any accurate reddening and distance estimates were available for most clusters in the inner 5° and consequently not much could be inferred about their spatial distribution (Racine & Harris 1989). We now have gathered CCD Colour-Magnitude Diagrams (CMD) data for 16 out of 17 known globular clusters within 5°, and these data make it possible to study the properties of this inner system. Most of these CMDs are now published with individual analyses of the clusters, and in the present work we complement them with some new results to build up the most homogeneous and updated set of information for this central sample.

Globular clusters are suitable probes to trace the bulge shape. In this work we address questions related to the spatial distribution of the globular clusters projected close to the Galactic center such as: are clusters detected on the far side of the Galaxy; how do the detected cluster distances compare with that of the Galactic center; what is the shape of this subsystem?

In Sect. 2 we determine the sample parameters. In Sect. 3 we discuss the results. Finally, in Sect. 4 the concluding remarks are given.

2. Parameters for globular clusters within the inner 5° radius

In order to study the spatial distribution of the inner bulge globular clusters, the required parameters are their reddening and implied distances. Such parameters are best derived from direct measurement *using magnitudes and colours of reference points in CMDs evolutionary sequences (horizontal branch – HB, bright giants – BG)*. An additional fundamental information is the metallicity which affects the reddening and distance derivations due to blanketing and temperature effects in the magnitudes and colours.

To illustrate the need for accurate parameters for the 17 central clusters, in Table 1 we report the distances given in the compilations of Webbink (1985), Peterson (1993) and Djorgovski (1993). Notice the discrepancy of distance values in some cases, and the several distance estimates placing clusters far on the other side of the Galaxy. E(B-V) and [Fe/H] from Racine & Harris (1989, hereafter RH89) are also indicated; we note that for most of these clusters the quality class III (very poor quality or no data) given in RH89 show the need for new observations, which is the concern of this paper.

⋆ Observations collected at the European Southern Observatory – ESO, Chile

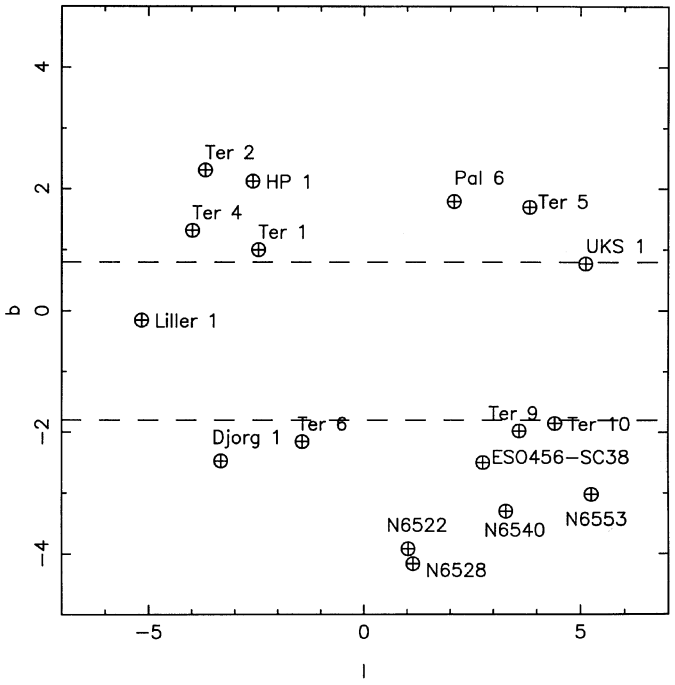

Fig. 1. Angular distribution of the sample clusters. The dashed lines represent the limit for cluster occurrence (except Liller 1).

Table 1. Distances $d_\odot$(kpc) for the sample clusters according to Webbink (1985) – W85, Peterson (1993) – P93 and Djorgovski (1993) D93, and parameters given in Racine & Harris (1989) – RH89.

cluster	$d_\odot$ W85	$d_\odot$ P93	$d_\odot$ D93	E(B-V) RH89	[Fe/H] RH89
Liller 1	7.9	–	7.9	2.8	+0.20
Terzan 4	16.1	16.9	16.9	1.53	-0.94
Terzan 2	10.0	2.1	10.0	1.42	-0.25
Djorg 1	–	–	26.3	1.2	–
HP 1	9.5	9.1	9.1	1.44	-0.56
Terzan 1	10.6	5.9	5.9	1.50	-0.71
Terzan 6	12.8	1.5	1.5	2.93	-0.61
NGC 6522	6.6	7.2	7.2	0.53	-1.04
NGC 6528	6.8	6.6	6.6	0.62	-0.23
Palomar 6	5.9	5.9	5.9	1.45	-0.74
ESO456 − SC38	–	–	3.8	1.2	–
NGC 6540	–	–	14.8	1.0	–
Terzan 5	7.1	14.6	7.9	1.92	-0.28
Terzan 9	7.0	13.8	13.8	1.48	-0.99
Terzan 10	14.6	–	–	1.7	–
UKS 1	10.4	–	10.4	3.07	-1.18
NGC 6553	5.7	3.5	3.5	0.80	-0.29

In the following we shall describe the derivation of parameters based on recent CCD photometry. We report homogeneously measured cluster parameters based on CCD images that we have collected at the 3.55m New Technology Telescope (NTT) and 1.54m Danish telescope at the *European Southern Observatory* (ESO), and with the Hubble Space Telescope – HST, in the last years. These data are in some cases complemented with sources from the literature, as indicated in the tables.

We show in Table 2 the 17 globular clusters which are projected within 5.2° of the Galactic center; NGC 6553 is projected at an angular radius of 6.0°, but it is included in the list because we have high quality HST data for this cluster. The Galactic coordinates are indicated in columns (2) and (3), whereas their angular distribution together with identifications are shown in Fig. 1. In this figure the dashed lines indicate limiting galactic latitudes where most clusters are located, except Liller 1. Notice the asymmetry between the northern and southern hemispheres, probably arising from the position of the Sun, which appears to be located at Z $\approx$ 20 pc above the galactic plane (Humphreys & Larsen 1995): our line of sight to the region around b $\approx$ -1° is far more reddened than that around b $\approx$ +1°.

2.1. Metallicities from CMDs

We deduced the metallicities by superimposing, on the studied CMDs, the mean loci of reference clusters (M30, NGC 6752 – see Rosino et al. 1997; 47 Tuc – Bica et al. 1994b); we also used for nearly solar metallicities the CMDs of NGC 6528 and NGC 6553 (Ortolani et al. 1995b) which are in the present sample. For NGC 6553 the metallicity was derived from high-resolution spectroscopy of individual giants (Barbuy et al. 1992). The metallicities of the template clusters are indicated in Table 3. Interpolation criteria for metal-rich clusters are as follows. Clusters of [Fe/H] $>$ -0.7 all show a red HB, almost superimposed on the RGB; besides, two other main CMD indicators are used: (i) the RGB curvature and extent can be used as a criterion to estimate the metallicities by means of the blanketing effects which causes cooler stars to become fainter (Ortolani et al. 1991); (ii) the magnitude difference between the HB level and the top (brightest stars) of the RGB (see Barbuy et al. 1997). We estimate a metallicity accuracy of $\pm$0.25 dex for metallicity determinations using the CMD criteria for this sample.

For Liller 1 we also took into account the metallicity estimation by Frogel et al. (1995) from JK photometry and Armandroff & Zinn (1988) from the integrated spectrum. For ESO456-SC38, Terzan 10 and UKS 1 the HB level was too close to the CMD limiting magnitude or below, and we used metallicities deduced from the CaII triplet measured in near-infrared integrated spectra obtained with the 2.15m CASLEO telescope in Argentina (Bica et al. 1998), as complementary information.

We show in Fig. 2 the CMDs of 3 clusters covering a range of metallicities: HP1 ([Fe/H] $\sim$ -1.5, Ortolani et al. 1997c), NGC 6553 ([Fe/H] $\sim$ -0.2, Ortolani et al. 1995b) and Terzan 5 ([Fe/H] $\sim$ 0.0, Ortolani et al. 1996a), for circular extractions of radius r $<$ 24", r $<$ 23" and r $<$ 42" respectively. We report in Table 2 (column 4) the revised metallicities based on the method described above.

2.2. Reddening and distance

The measurements on the CMDs consist of the V and I magnitudes of the HB and BGs, as well as the (V-I) colour of the

Table 2. Basic data for the sample clusters estimated from the measurement of bright giants (BG) combined to CMD mean loci of reference clusters. References to the table: 1 Ortolani et al. (1996b); 2 Frogel et al. (1995); 3 Ortolani et al. (1997a); 4 Ortolani et al. (1997b); 5 Ortolani et al. (1995a); 6 Ortolani et al. (1997c); 7 Ortolani et al. (1993a); 8 Barbuy et al. (1997); 9 Barbuy et al. (1992); 10 Terndrup & Walker (1994); 11 Ortolani et al. (1992); 12 Ortolani et al. (1995b); 13 Ortolani et al. (1997d); 14 Bica et al. (1998); 15 Bica et al. (1994a); 16 Ortolani et al. (1996a); 17 Guarnieri et al. (1998)

cluster	l°	b°	[Fe/H]	V_{HB}	I_{HB}	V_{BG}	I_{BG}	$(V\text{-}I)^{HB}_{RGB}$	E(V-I)	$\frac{E(V-I)}{E(B\text{-}V)}$	E(B-V)	ref
(1)	(2)	(3)	(4)	(5)	(6)	(7)	(8)	(9)	(10)	(11)	(12)	(13)
Liller 1	-5.16	-0.16	+0.2	–	–	–	18.0 ±0.25	–	–	1.35	3.0	1,2
Terzan 4	-3.98	+1.31	-2.0:	22.4 ±0.15	19.0 ±0.15	19.0 ±0.3	14.7 ±0.3	3.86 ±0.15	3.05	1.32	2.31	3
Terzan 2	-3.68	+2.30	-0.5 ±0.12	20.3 ±0.12	17.4 ±0.1	18.1 ±0.15	14.7 ±0.06	3.04	2.06	1.32	1.56	4
Djorg 1	-3.33	-2.48	-0.4 ±0.25	20.8 ±0.25	17.5 ±0.2	18.65 ±0.15	15.1 ±0.12	3.27	2.24	1.32	1.70	5
HP 1	-2.58	+2.11	-1.5	18.6 ±0.08	16.8 ±0.12	16.25 ±0.1	13.37. ±0.12	2.5 ±0.06	1.57	1.30	1.21	6
Terzan 1	-2.44	+0.99	+0.2	–	–	19.0	14.0	–	–	–	1.67	7
Terzan 6	-1.43	-2.16	-0.5	22.3 ±0.12	18.45 ±0.12	20.25 ±0.2	14.75 ±0.2	3.98 ±0.08	3.0	1.33	2.26	8
NGC 6522	+1.03	-3.93	-1.3	16.4 ±0.2	15.4 ±0.12	14.0 ±0.2	12.0 ±0.2	1.60 ±0.1	–	1.29	0.55	9,10
NGC 6528	+1.14	-4.18	-0.2	17.2 ±0.15	15.4 ±0.12	15.7 ±0.3	12.2 ±0.3	1.83 ±0.1	0.68	1.31	0.52	11,12
Palomar 6	+2.09	+1.78	-0.4	19.6 ±0.25	16.8 ±0.2	16.9 ±0.2	13.3 ±0.2	2.82 ±0.12	1.79	1.32	1.36	5
ESO 456 −SC38	+2.76	-2.51	-0.5	17.6*	–	15.5 ±0.2	12.7 ±0.2	2.2 ±0.15	1.18	1.31	0.90	13,14
NGC 6540	3.28	-3.31	-1.0	15.1 ±0.3	–	–	–	–	–	1.29	0.60	15
Terzan 9	+3.60	-1.99										
Terzan 5	+3.84	+1.69	0.0	22.48 ±0.25	18.2 ±0.2	20.25 ±0.2	14.8 ±0.2	4.4 ±0.15	3.23	1.35	2.39	16
Terzan 10	+4.42	-1.86	-1.0	21.9*	–	19.7 ±0.2	15.2 ±0.2	4.0 ±0.15	3.2	1.32	2.41	13,14
UKS 1	+5.12	+0.76	-0.5	–	–	–	17.5 ±0.2	–	–	1.35	3.1	13,14
NGC 6553	+5.25	-3.03	-0.2 ±0.1	16.92 ±0.1	14.9 ±0.1	15.25 ±0.1	12.2 ±0.04	2.15	0.95	1.31	0.7	12,17

red giant branch (RGB) at the HB level ($(V\text{-}I)^{HB}_{RGB}$). Given that the cluster sample spans a wide range of reddening values, for some of them we can measure all these magnitudes and colours, whereas for the most obscured ones we dispose only of the I magnitude of the bright giants. For NGC 6540 and NGC 6522 we dispose of B and V photometry only, where their HBs are defined, but the RGB is underpopulated, so that we only have V_{HB}.

For most of the sample the E(V-I) reddening could be determined. We derived it from the difference of the observed $(V\text{-}I)^{HB}_{RGB}$ to the intrinsic values of well-studied reference clusters as a function of metallicity, as reported in Table 3.

For the subsequent analysis we converted E(V-I) into E(B-V), mainly because the total-to-selective absorption R is better known in terms of E(B-V). The ratio E(V-I)/E(B-V) depends on the cluster metallicity and on the amount of reddening. Eq. A1 of Dean et al. (1978) was used, and the resulting ratios for each cluster are listed in Table 2, together with the calculated E(B-V). In the case of NGC 6540 and NGC 6522 we disposed of direct B, V estimates of E(B-V).

The steps to derive cluster distances are reported in Table 4. We adopted a total-to-selective absorption $R = A_V/E(B\text{-}V)$ dependent on the effective wavelength shift of the filters. The adoption of a constant value would be an oversimplification; this dependence can be neglected in the halo but not in low latitude bulge fields, due to a high reddening and in many cases a high 0.05metallicity. Small changes in R imply large distance variations – see for example the discussion on Terzan 6 (Barbuy et al.

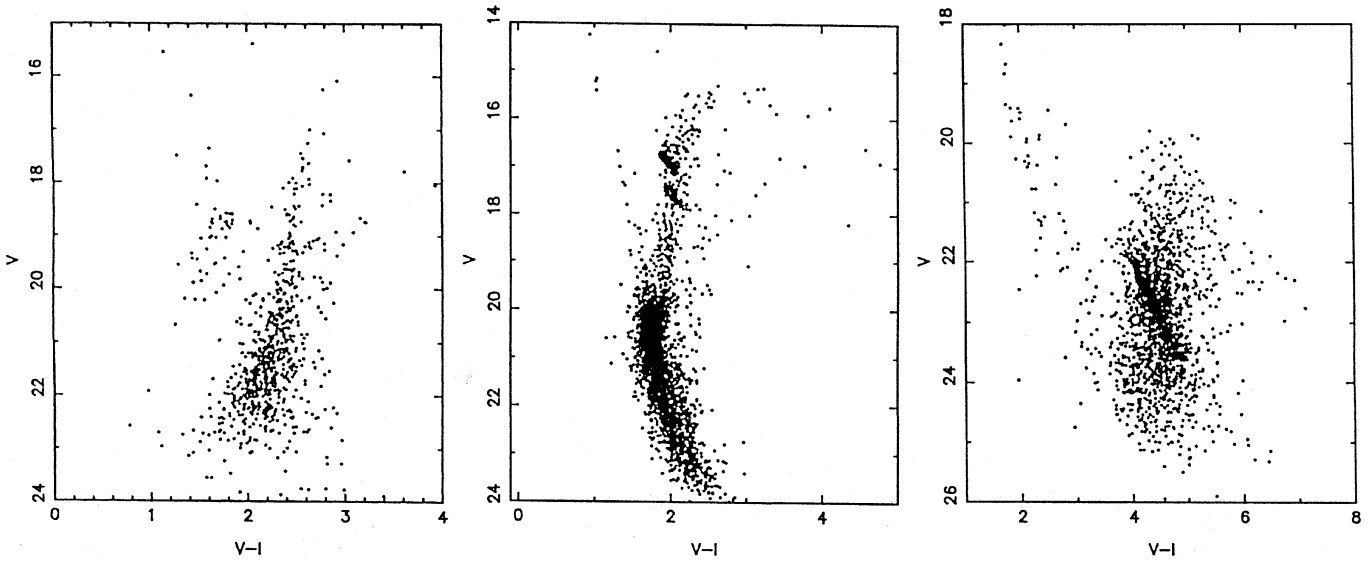

Fig. 2. Colour-magnitude diagrams of HP1 ([Fe/H] $\sim$ -1.5), NGC 6553 ([Fe/H] $\sim$ -0.2) and Terzan 5 ([Fe/H] $\sim$ 0.0), for circular extractions of radius r $<$ 24", r $<$ 23" and r $<$ 42" respectively.

1997). In fact, R is a fundamental scaling factor for distances in the Galaxy, when optical observations are used. Following the results by Grebel & Roberts (1995) for the metallicity dependence of R, we adopted R = 3.6 for the most metal-rich clusters in our sample, and R = 3.1 for [Fe/H] $\leq$ -1.0 (see also Terndrup 1988), and intermediate values were linearly interpolated. Besides, we adopted the reddening dependence of R on E(B-V) as given in Olson (1975): ΔR = 0.05E(B-V). The resulting R+ΔR and A_V values are given in Table 4.

Absolute magnitudes of the horizontal branch M_V^{HB} are metallicity dependent. We adopted Jones et al. (1992)'s relation, slightly modifying the zero point in order to fit the results by Guarnieri et al. (1998) for NGC 6553: M_V^{HB} = 0.16[Fe/H] + 0.98. For two sample clusters which are extremely reddened (Liller 1 and UKS1) the HB level was not measurable, so that we relied on the bright giants I magnitudes. So, we used the ratio A_I/A_V = 0.61 and the absolute I magnitude of the brightest giants M_I^{BG} = -3.2; the latter value is a mean derived from our best CMDs for metal-rich clusters (NGC 6528, NGC 6553, Terzan 2, Terzan 5, Terzan 6). The observed and absolute distance moduli are shown in columns 5-6 of Table 4, together with those for the remainder clusters obtained from M_V^{HB}.

Finally, the distances from the Sun $d_\odot$ and Galactocentric Y and Z projections, together with their heliocentric projected distance $X_\odot$ are given in columns 7–10 of Table 4.

2.3. Errors

The zero point accuracy of the standard star equations is estimated to be about $\pm$0.03 magnitudes. The final accuracy of our calibrations is dominated by crowding effects in the aperture photometry required for the magnitude transfer from the cluster images to the standard stars. From a comparison with the theoretical growth curves and our measurements we estimate that this source of error can amount to about 0.05 mag. However, larger systematic errors cannot be excluded. Also the relative photometry is largely dominated by crowding and therefore it is a function of the relative position with respect to the cluster centers. From frame to frame comparisons we estimated a typical average error of about 0.02 mag. down to I=17.5; for fainter magnitudes it rapidly increases to 0.07 at I=18.5 (see references for individual cluster CMD analyses in Table 2). This error corresponds to the photon noise and pixel instabilities; it can be considered as a lower limit since it was derived from images having very similar crowding. More details on photometry obtained in crowded fields in the galactic bulge are discussed in Ortolani et al. (1990, 1992, 1993a, 1996b).

An important source of error in our distance moduli comes from the spread in the CMD features (HB, RGB), mainly due to crowding, differential reddening and field contamination. Typically they are $\pm$0.15 mag. for the HB level and $\pm$0.03 in colour for the RGB at the HB level. When only bright giants are available the magnitude uncertainty may amount to $\pm$0.25 in such clusters.

Table 3. $(V\text{-}I)^{HB}_{RGB}$ colour of the giant branch at the horizontal branch level for well studied clusters in the whole range of metallicities. References indicated as superscripts: 1 Zinn (1985); 2 Bica et al. (1994b); 3 Barbuy et al. (1992); 4 Rosino et al. (1997); 5 Guarnieri et al. (1998); 6 Ortolani et al. (1992); 7 Webbink (1985)

cluster	[Fe/H]	(V-I)	E(B-V)	E(V-I)	$(V\text{-}I)_o$
M 30	-2.13[1]	0.89[4]	0.06[7]	0.08[7]	0.81
NGC 6752	-1.54[1]	1.00[4]	0.05[7]	0.07[7]	0.93
47 Tuc	-0.71[1]	1.00[2]	0.04[7]	0.05[7]	0.95
NGC 6356	-0.40[2]	1.30[2]	0.24[2]	0.32[2]	0.98
NGC 6553	-0.20[3]	2.15[5]	0.7[5]	0.95[5]	1.20
NGC 6528	-0.20[3,6]	1.83[6]	0.55[6]	0.73[6]	1.10

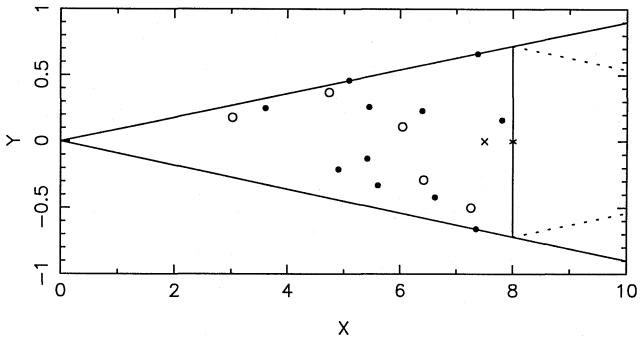

Fig. 3. $X_\odot$, Y projection of the sample clusters. Symbols: ⊙: Sun, and Galactic center positions according to +: Reid (1993), x: Racine & Harris (1989). Dots are metal-rich globular clusters; open circles are metal-poor ones ([Fe/H] $\leq$ -0.8). The field of view is shown, together with its counterpart on the far side (dotted area).

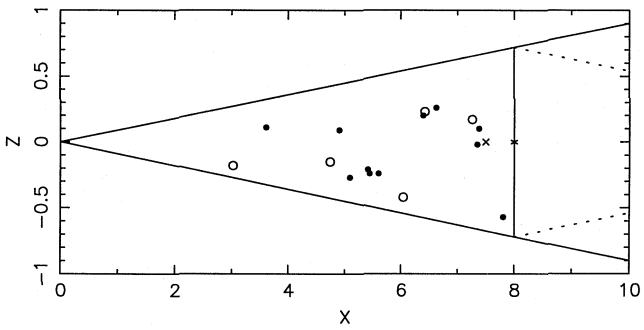

Fig. 4. Same as Fig. 3 for the $X_\odot$, Z plane.

Uncertainties associated to the total-to-selective absorption R are the dominant ones, estimated to be δ(R) $\approx \pm 0.2$, which imply typical errors of 10% in distance for E(B-V) = 1.0, but rapidly increasing with the reddening. This corresponds to $\pm$0.23 in magnitudes.

An additional uncertainty comes from the slope of the relation between the absolute magnitude of the HB M_V^{HB} vs. [Fe/H] (Buonanno et al. 1989; Fusi Pecci et al. 1990). For the metallicity distribution of our sample clusters we infer δ(Fe) $\approx \pm 0.3$, which results in $\delta(M_V^{HB}) \approx \pm 0.3$. If we consider the possibility of a systematic change on the zero point of the M_V^{HB} based on recent Hipparcos data, the whole distance scale of the present sample would change accordingly.

Therefore, considering the errors due to (a) zero point photometric calibration, (b) photometric spread on the CMD, (c) uncertainty in the selective-to-total absorption R, (d) slope of the M_V^{HB} vs. [Fe/H] relation, we end up with an uncertainty in distance modulus of $\pm$0.28 mag, or $\approx$ 13% in distance.

3. Discussion

The use of CCD detectors considerably improved the knowledge of distances for this inner bulge sample (Table 1 vs. Table 4).

We show in Figs. 3 and 4 the projected cluster positions in the $X_\odot$, Y and $X_\odot$, Z planes, where the positions of the Galactic center according to Reid (1993) and Racine & Harris (1989), respectively of $d_\odot^{G.C.}$ = 8.0 and 7.5 kpc, are also indicated. As a check of the distance method applied in Sect. 2.2 we have estimated the distance of the Galactic center using Baade's Window CMDs by Terndrup (1988), following the same procedures adopted in the present paper. We obtained E(B-V) = 0.46, a total-to-selective absorption R = 3.6, and a distance $d_\odot^{G.C.}$ = 7.85$\pm$0.2 kpc, in agreement with the estimates above for the Galactic Center.

No clusters are seen beyond 8 kpc from the Sun in the analysed solid angle. This conclusion is new relative to previous compilations (Webbink 1985; Racine & Harris 1989). The absence can be explained taking into account the fact that in Fig. 1 there is evidence of a heavy extinction strip of $\approx$2.5° wide in the Z direction, where essentially all possible clusters are blocked from view. This angle of view corresponds to Z $\approx$ 330 pc at the distance of the Galactic Center (assuming 8 kpc for the distance). This value encompasses 14 of the 16 sample clusters (Table 4).

The missing clusters on the opposite side of the Galaxy, may amount to $\sim$ 15 in an equivalent solid angle, from symmetry arguments, assuming $d_\odot^{G.C.}$ = 8.0 kpc. Infrared surveys may detect such globular clusters.

A 3D combination of Figs. 3 and 4 (see also Table 4) suggests that there occurs an empty zone inside a radius of about $\approx$ 0.7 kpc (with only one exception which is however $\approx$ 0.6 kpc below the Galactic plane – see Fig. 4). In fact, a zone of avoidance is dynamically expected (Harris 1990). It is interesting to note that 55% of the sample clusters are post core-collapse (Trager et al. 1995). This fraction is considerably higher than the 15% of all remainder Galactic clusters, excluding the present sample.

This suggests that only such very concentrated clusters would have survived to tidal disruption and disk shocking in the central bulge.

In Figs. 3 and 4 we separate the sample into metal-rich ([Fe/H] $\geq$ -0.8) and metal-poor clusters. There is no evidence for segregation between the two groups. In Y, these globular clusters occupy the entire solid angle, whereas most clusters are located at Z $<$ 250 pc. This information, combined to the depth ($X_\odot$) distribution would favour a flattened central bulge, extending to $d_\odot \approx$ 4.5 kpc.

We show in Fig. 5 V_{HB} vs. E(B-V). The correlation is quite strong corresponding to an average slope R $\approx$ 3.4. This clearly shows that a constant low value R = 3.1, as often adopted, is not appropriate for the bulge clusters.

In Fig. 6 we show $d_\odot$ vs. E(B-V), where there is no correlation, in particular we see clusters having the same reddening at significantly different distances. We conclude that reddening effects on the observed level of the HB prevail over depth effects (distance). This is due to the small thickness of the dust layer in the disk, as compared to the scale height (z) of our clusters relative to the Galactic plane. In fact, even at |b| = 1.5° the line of sight crossing a dust layer with scale height of 80 pc is limited to $\approx$ 2.5 kpc, which is less than the nearest cluster to the Sun observed in our sample. Hence, the reddening arises mostly in the local dust clouds.

Table 4. Parameters for distance derivation: R = A_V/E(B-V), visual extinction A_V, absolute magnitude of the horizontal branch M_V^{HB}, observed and dereddened distance modulus, distance to the Sun, heliocentric projected distance $X_\odot$ and Galactocentric Y and Y projections. (a) the I magnitude was employed; (b) for UKS 1 we adopted as reference the average bright giants of 47 Tuc (Bica et al. 1994b), M_I = -3.39.

cluster (1)	R (2)	A_V (3)	M_V^{HB} (4)	(V-M_V) (5)	(m-M)$_o$ (6)	$d_\odot$(kpc) (7)	$X_\odot$ (8)	Y (9)	Z (10)
Liller 1	3.75	11.25	–	25.59[a]	14.34	7.38	7.35	-0.66	-0.02
Terzan 4	3.22	7.44	0.66	21.75	14.31	7.28	7.26	-0.50	+0.17
Terzan 2	3.39	5.29	0.9	19.4	14.11	6.64	6.62	-0.42	+0.26
Djorg 1	3.44	5.85	0.92	19.6	13.75	5.62	5.60	-0.33	-0.24
HP 1	3.16	3.82	0.74	17.86	14.04	6.43	6.42	-0.29	+0.23
Terzan 1	3.68	6.15	–	19.60[a]	13.45	4.90	4.90	-0.21	+0.09
Terzan 6	3.42	7.73	0.9	21.4	13.67	5.42	5.41	-0.13	-0.21
NGC 6522	3.13	1.72	0.77	15.63	13.91	6.05	6.04	+0.11	-0.42
NGC 6528	3.46	1.80	0.95	16.25	14.45	7.83	7.81	+0.16	-0.57
Palomar 6	3.42	4.65	0.92	18.68	14.03	6.40	6.39	+0.23	+0.20
ESO456 − SC38	3.35	3.02	0.90	16.7	13.68	5.45	5.44	+0.26	-0.24
NGC 6540	3.13	1.88	0.82	14.28	12.40	3.02	3.02	+0.18	-0.18
Terzan 5	3.64	8.70	0.98	21.5	12.80	3.63	3.61	+0.25	+0.11
Terzan 10	3.22	7.77	0.74	21.16	13.39	4.76	4.74	+0.37	-0.15
UKS 1	3.46	10.73	–	25.08[a,b]	14.35	7.41	7.38	+0.66	+0.10
NGC 6553	3.47	2.43	0.95	15.97	13.54	5.10	5.09	+0.46	-0.27

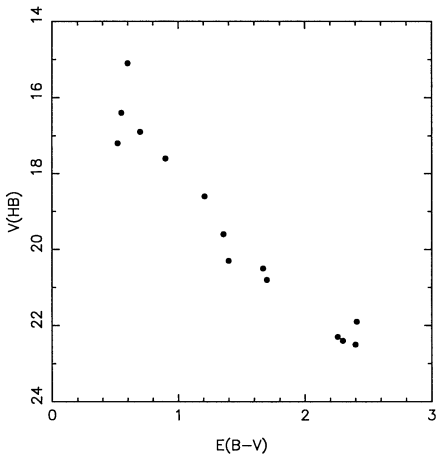

Fig. 5. Observed horizontal branch level (V_{HB} vs. reddening E(B-V).

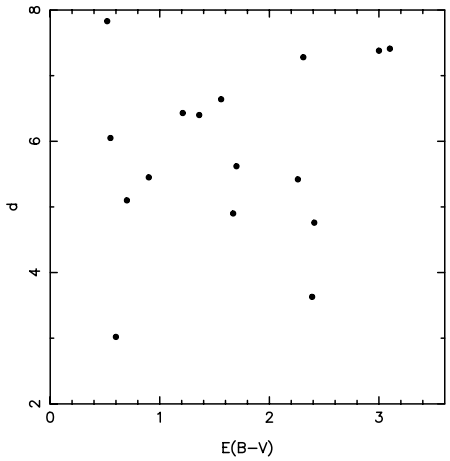

Fig. 6. Distance from the Sun ($d_\odot$) in kpc vs. reddening E(B-V).

Fig. 7 shows the reddening against the Galactic latitude |b|. The data are binned in 1° intervals. Circles indicate southern clusters, northern ones are indicated by crosses. It appears that southern clusters are on average more extinguished than northern ones, consistent with the current interpretation that the Sun lies above the Galactic plane by ≈ 20 pc (see also Fig. 1). However, bulge windows with low extinction are well known to be in the southern galactic hemisphere. This is not in contradiction with the above discussion, because the dust is distributed in discrete clouds, and the distribution of local dust clouds probably causes the windows.

From Figs. 1 and 7 it is possible to estimate the height of the Sun above the Galactic plane. Comparing the absorption in the southern and northern Galactic hemispheres it is clear that: (i) the latitute detection limit in the south is about 3 times that in the north; (ii) at the same latitude the color excess difference is ΔE(B-V) ≈ 0.40-0.50 mag, corresponding to a flux attenuation of a factor ≈3.6. Because of the absence of correlation between reddening and distance (Fig. 6) and given the distances from the plane for our clusters to be mostly in the range 100 < Z < 250 pc (Table 4), the absorption arises in a layer of less than 100 pc within a few kpc from the Sun. This value is in agreement with classical estimates of the gas and dust scale heights of ≈ 80 pc (Burton 1976; Combes 1991). Assuming an exponential decrease of the dust density, the Sun must be located ≈ 10-15 pc above the Galactic plane, a value comparable with estimates from other methods (see Humphreys & Larsen 1995 for a recent review).

In Fig. 8 we show the projection of our sample clusters on the disk, where the ellipse representing the bar according to Blitz & Spergel (1991) is also plotted. No clear evidence for such bar

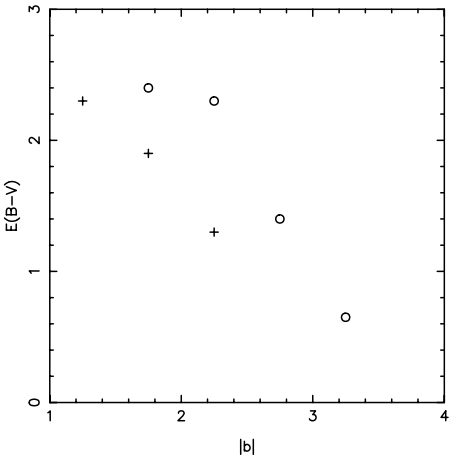

Fig. 7. Reddening E(B-V) binned into 1° Galactic latitude steps againt |b|. Circles are for southern galactic hemisphere clusters, and crosses are northern ones.

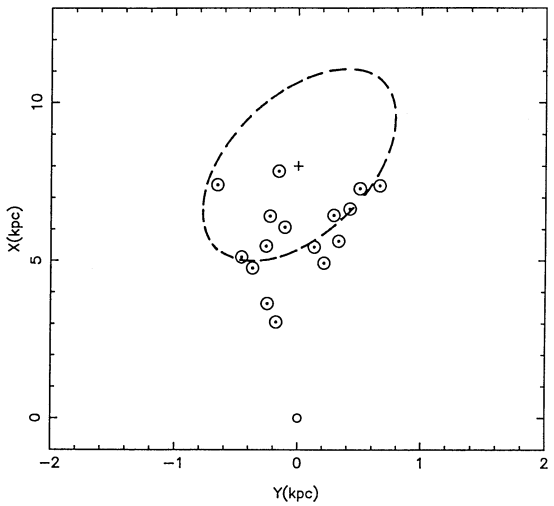

Fig. 8. Projection on the disk of the sample globular clusters. The ellipse corresponds to the outer contours of the bar as proposed by Blitz & Spergel (1991). The position of the Sun and Galactic center are also indicated.

is seen in the cluster distribution. In order to decide whether the clusters are distributed in a bar or not, it would be necessary to extend the CMD parameter studies to a wider solid angle. We note that Alcock et al. (1997) found a bar-like distribution for RGB-clump stars whereas the bulk of RR Lyrae in the same fields is not barred.

We emphasize that the present globular clusters form a distinct population from that discussed by Armandroff (1989), because the present scale height is about a factor of ≈ 3 smaller. We show in Fig. 9 the distribution in Z of the present sample, compared to that of Armandroff's sample. It is clear that the distribution of the present sample is much more internal, and compatible with Kent's (1991) bulge exponential distribution (see Fig. 2 of Rich 1993).

The metallicity histogram for this central bulge sample, based on the CMD morphology (Table 2), is shown in Fig. 10.

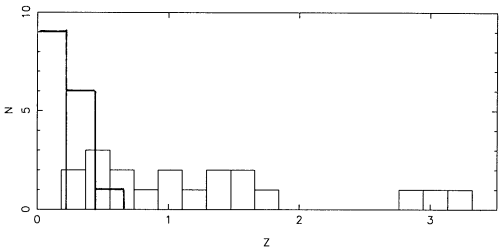

Fig. 9. Histogram of height from the Galactic plane Z: present sample (solid line), Armandroff's (1989) sample (strong solid line).

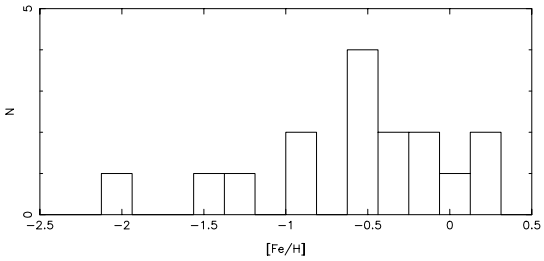

Fig. 10. Metallicity histogram for the present sample.

The distribution is quite flat and broad extending from about twice solar to less than one tenth solar abundance (some halo clusters may be contaminating the sample). The sample is small but resembles that of bulge stars (McWilliam & Rich 1994). Recently, Ortolani et al. (1995b), using *Hubble Space Telescope* (HST) data of NGC 6528 and NGC 6553, two metal-rich globular clusters with a CMD morphology comparable to that of Baade's Window (see their Fig. 3), favour an old age for the bulge. Combining the latter dating result with those from the present paper about the spatial distribution based on high-quality ground-based optical photometry for essentially the whole sample of inner globular clusters, the picture which comes out is one of a flat old central bulge, with a common origin for the stellar population of both globular clusters and field stars.

4. Concluding remarks

The present revision of metallicities and spatial distributions based on new observations bring closer the properties of central globular clusters to those of bulge field stars. These results along with the evidence of ages for NGC 6553 and NGC 6528 comparable to halo clusters (Ortolani et al. 1995b), point to an old flattened bulge extending to 4.5 kpc from the Sun. In turn, this indicates fundamental constraints on the models of the formation and early evolution of the Galaxy. More main sequence photometry for this inner sample with Hubble Space Telescope or other high-quality imaging instrument is of course necessary to further test and constrain this scenario.

Acknowledgements. We are grateful to R. M. Rich for helpful comments. BB and EB acknowledge partial financial support from CNPq and Fapesp.

References

Alcock, C. et al. (The MACHO collaboration) 1997, ApJ, submitted
Armandroff, T. 1989, AJ, 97, 375
Armandroff, T., Zinn, R. 1988, AJ, 96, 92
Barbuy, B., Castro, S., Ortolani, S., Bica, E. 1992, A&A, 259, 607
Barbuy, B., Ortolani, S., Bica, E. 1997, A&AS, 122, 483
Bica, E., Clariá, J.J., Piatti, A.E., Bonatto, C. 1998, A&A, submitted
Bica, E., Ortolani, S. & Barbuy, B. 1994a, A&A, 283, 67
Bica, E., Ortolani, S. & Barbuy, B. 1994b, A&AS, 106, 161
Blitz, L., Spergel, D.N. 1991, ApJ, 379, 631
Buonanno, R., Corsi, C.E., Fusi Pecci, F. 1989, A&A, 216, 80
Burton, W.B. 1976, ARA&A, 14, 275
Combes, F. 1991, ARA&A, 29, 195
Dean, J.F., Warpen, P.R., Cousins, A.J. 1978, MNRAS, 183, 569
Djorgovski, S. 1993, ASP Conf. Ser. 50, p. 373
Frogel, J.A., Kuchinski, L.E., Tiede, G.P. 1995, AJ, 109, 1154
Fusi Pecci, F., Ferraro, F.R., Crocker, D.A., Rood, R.T., Buonanno, R. 1990, A&A, 238, 95
Grebel, A.K., Roberts, W. 1995, A&AS, 109, 293
Guarnieri, M.D., Ortolani, S., Montegriffo, P., Renzini, A., Barbuy, B., Bica, E., Moneti, A. 1998, A&A, 331, 70
Harris, W.E. 1990, in Bulges of Galaxies, eds. B.J. Jarvis & D. Terndrup, ESO Conf. Workshop Proc. no 35, p. 153
Humphreys, R. M., Larsen, J. A. 1995, AJ, 110, 2183
Jones, R.V., Carney, B.W., Storm, J., Latham, D.W. 1992, ApJ, 386, 646
Kent, S.M., Dame, T.M., Fazio, G. 1991, ApJ, 378, 131
Larson, R.B. 1990, PASP, 102, 709
McWilliam, A., Rich, R.M. 1994, ApJS, 91, 749
Minniti, D. 1995, AJ, 109, 1663
Olson, B.I. 1975, PASP, 87, 349
Ortolani, S., Barbuy, B. & Bica, E. 1990, A&A, 236, 362
Ortolani, S., Barbuy, B. & Bica, E. 1991, A&A, 249, L31
Ortolani, S., Barbuy, B., Bica, E. 1996a, A&A, 308, 733
Ortolani, S., Barbuy, B., Bica, E. 1997a, A&A, 319, 850
Ortolani, S., Bica, E., Barbuy, B. 1992, A&AS 92, 441
Ortolani, S., Bica, E. & Barbuy, B. 1993a, A&A, 267, 66
Ortolani, S., Bica, E., Barbuy, B. 1993b, A&A, 273, 415
Ortolani, S., Bica, E., Barbuy, B. 1995a, A&A, 296, 680
Ortolani, S., Bica, E. & Barbuy, B. 1996b, A&A, 306, 134
Ortolani, S., Bica, E., Barbuy, B. 1997b, A&A, 326, 614
Ortolani, S., Bica, E. & Barbuy, B. 1997c, MNRAS, 284, 692
Ortolani, S., Bica, E., Barbuy, B. 1997d, A&AS, 126, 319
Ortolani, S., Renzini, A., Gilmozzi, R., Marconi, G., Barbuy, E., Bica, E. & Rich, R.M. 1995b, Nature, 377, 701
Peterson, C.J. 1993, ASP Conf. Ser. 50, p. 337
Racine, R., Harris, W.E. 1989, AJ, 98, 1609
Raha, N., Sellwood, J.A., James, R.A., Kahn, F. D. Nature, 352, 411
Reid, M. 1993, ARA&A, 31, 345
Rich, R.M. 1993, ASP Conf. Ser. 48, 287
Rosino, L., Ortolani, S., Barbuy, B., Bica, E., 1997, MNRAS, 289, 745
Spergel, D.N., Malhotra, S., Blitz, L. 1996, in Spiral Galaxies in the Near-IR, eds. D. Minniti, H.-W. Rix, Springer-Verlag,p. 128
Terndrup, D.M. 1988, AJ, 96, 884
Terndrup, D.M., Walker, A.R. 1994, AJ, 107, 1786
Trager, S.C., King, I.R. & Djorgovs.ki, S. 1995, AJ, 109, 218
Webbink, R.F. 1985, in Dynamics of Star Clusters IAU Symp. 113, eds. J. Goodman & P. Hut, (Dordrecht: Reidel), p. 541
Zinn, R. 1985, ApJ, 293, 424